Proceedings of the 2006 American Control Conference
Minneapolis, Minnesota, USA, June 14-16, 2006

Exploiting $\mathcal{H}_\infty$ Sampled-Data Control Theory for High-Precision Electromechanical Servo Control Design

Tom Oomen, Marc van de Wal, and Okko Bosgra

Abstract— **Optimal design of digital controllers for industrial electromechanical servo systems using an $\mathcal{H}_\infty$-criterion is considered. Present industrial practice is to perform the control design in the continuous time domain and to discretize the controller *a posteriori*. This procedure involves unnecessary approximations. Alternatively, a direct sampled-data control design can be made, where an optimal discrete time controller is computed for a continuous time standard plant. Though theoretically and numerically solvable, a sampled-data approach is hardly feasible in an industrial environment. In this paper, a discrete time control design approach is taken. Tools that stem from sampled-data control and multirate systems theory are presented to evaluate the intersample behavior in the frequency domain, since intersample behavior is not explicitly addressed during discrete time control design. Experimental results are given to illustrate the effectiveness of the proposed discrete time control design approach and to illustrate the importance of intersample behavior in practical applications.**

I. Introduction

Industrial high-precision electromechanical servo systems are subject to increasing demands regarding speed and performance. An example of such a system is a wafer stage, that is part of a wafer scanner. Wafer scanners are used for the production of Integrated Circuits (ICs), see [22]. Besides a perfect electromechanical design, an appropriate control system is required to meet these ever increasing demands. Recently, advanced control design tools based on $\mathcal{H}_\infty$-optimization have successfully been applied to wafer stages [25]. The key to success is that $\mathcal{H}_\infty$-optimization can handle MIMO plants, it can deliver robust controllers, and the design can be based on loopshaping techniques.

Traditionally, both the theory required for $\mathcal{H}_\infty$-optimization [9] and industrial control design tools have been developed in the continuous time domain. Performing the control design in the continuous time domain is most natural, since the electromechanical system evolves in continuous time. The resulting controller, however, is typically implemented in a digital environment because of high flexibility. The discrete time controller operates at a prescribed sampling frequency due to computational and economical reasons. The conversion of a continuous time controller into the discrete time domain often involves an approximation [11].

T. Oomen and O. Bosgra are with the Faculty of Mechanical Engineering, Control Systems Technology, Technische Universiteit Eindhoven, 5600 MB Eindhoven, The Netherlands t.a.e.oomen@tue.nl, o.h.bosgra@tue.nl

M. van de Wal is with Philips Applied Technologies, Mechatronics Technologies, Acoustics & Control, 5600 MD Eindhoven, The Netherlands m.m.j.van.de.wal@philips.com

In the last decade, $\mathcal{H}_\infty$ optimal control theory has been further extended to handle both discrete time [12] and sampled-data systems [4], [7]. Sampled-data control design solves the true control goal: the design of a discrete time controller for a continuous time plant with appropriate Analog-Digital (AD) and Digital-Analog (DA) converters and continuous time performance specifications. The present state of affairs in industry is still a continuous time control design with *a posteriori* controller discretization. Due to increasing demands regarding speed and accuracy, explicitly accounting for the digital controller implementation is inevitable in high-performance industrial applications.

A sampled-data approach is not yet feasible in an industrial control design procedure, since an accurate continuous time model of the system is required. Such models are not straightforward to obtain in practice [19]. Also, addressing Linear Time Invariant (LTI) uncertainty results in a large computational burden [10] and a loopshaping-based design is not straightforward. In this paper, a control design approach is taken, where:

- a discrete time $\mathcal{H}_\infty$ control design is performed, based upon a model of the electromechanical system as seen from the digital computer. Consequently, performance is specified *at* the controller sampling instants. No approximations are present in the design procedure.
- the intersample response, *i.e.*, the response of the electromechanical system *in between* the controller sampling instants, is evaluated *a posteriori* to control design. This step requires a discrete time plant model at a higher sampling frequency or a continuous time plant model. The former results in a sampled-data analysis problem, whereas the latter results in a multirate analysis problem. If the intersample behavior is not satisfactory, the discrete time control design will be improved iteratively.

The remainder of this paper is organized as follows. In Section II, a continuous time control design approach based on $\mathcal{H}_\infty$-optimization/μ-synthesis is reviewed that has successfully been applied to high precision motion systems. In Section III, a discrete time control design approach is presented that extends the approach in Section II in the sense that the digital controller implementation is explicitly addressed. In Section IV, sampled-data control theory is briefly reviewed. It is argued that sampled-data control design does not fit into a high-precision industrial control design approach. Several tools from sampled-data and multirate control are exploited to analyze the intersample response of the system to exogenous inputs. In Section V, experimental results are given to demonstrate the effectiveness of

1-4244-0210-7/06/$20.00 ©2006 IEEE

the proposed discrete time control design approach and to illustrate the importance of intersample behavior in practical applications. For ease of presentation, only the SISO case is considered, extensions to the MIMO case are conceptually straightforward, see [25].

II. Control Design for High-Precision Industrial Applications

A review of a continuous time control design procedure is given that uses $\mathcal{H}_\infty$-optimization/μ-synthesis. The setup of Fig. 1 is used throughout this section. Here, w is the vector of (weighted) exogenous inputs, *e.g.*, reference signals and disturbances, z is the vector of (weighted) exogenous outputs, *e.g.*, actuator and error signals, u is the vector of manipulated variables and y is the vector of measured variables. Furthermore, G_c denotes the continuous time standard plant that contains a continuous time plant model P_c and appropriate weighting filters, and K_c denotes a continuous time controller. Throughout this paper, all models are assumed to be LTI.

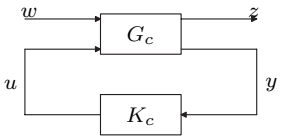

Fig. 1. Continuous time standard plant.

A. Design Procedure

A stepwise approach is summarized that enables the design of high-performance MIMO controllers for electromechanical systems. The design procedure is often performed iteratively. For a more detailed exposition and assumptions regarding the plant P_c, see [25].

1) *Control goal and structure:* define exogenous inputs w and exogenous outputs z. Moreover, define the measured variables y and manipulated variables u.
2) *Plant modeling:* model the plant as a continuous time finite dimensional LTI system. Either physical modeling [17] or System Identification (SI) techniques [16] can be used. SI is most useful for electromechanical systems, since it enables an accurate identification of parasitic, flexible dynamics and experimentation is relatively cheap. Furthermore, the frequency domain is used for SI, since this has several advantages over a time domain aproach, see [18]. Reduce the order of the plant if necessary, see, *e.g.*, [26].
3) *Control goal quantification:* quantify the control goal by means of frequency domain weighting filters. The proposed weighting filters in [25] resemble manual loopshaping ideas, see also [21]. Specifically, bounds are defined for closed-loop transfer function matrices, *e.g.*, the sensitivity function $S(s)$. These weighting filters are incorporated in the standard plant G_c.
4) *Model uncertainty quantification:* this optional step enables the designer to explicitly incorporate an uncertainty model in the control design procedure by introducing fictitious exogenous inputs and outputs.
5) *Controller synthesis:* compute
$$K_c = \arg\min_{K_c} \|\mathcal{F}_l(G_c, K_c)\|_\infty, \tag{1}$$
e.g., by using a commercially available toolbox [3]. If the order of the resulting controller is too high, reduce its order to enable real-time implementation [26].
6) *Controller discretization:* the controller resulting from Step 5 is typically a continuous time controller that should be discretized to enable digital implementation.

B. Shortcomings

The approach in Section II-A has two shortcomings. Firstly, Step 2 is not straightforward. The data used for SI are collected on a digital computer. The resulting model is then a discrete time one. Without any further assumptions on the underlying continuous time plant, it is not possible to reconstruct an accurate continuous time model from a discrete time model [8], [19]. Secondly, Step 6 typically involves an approximation [11]. The approximation error reduces if the sampling frequency is increased. In practice, however, the sampling frequency is upper bounded due to computational and economical reasons and an approximation error is inevitable.

III. A Step Towards Discrete Time Control

A discrete time control design approach is presented that does not have the deficiencies of Section II-B. The proposed approach makes use of the bilinear transformation that is elaborated on first. Then, a stepwise approach is presented that is similar to Section II.

A. Uniting Continuous and Discrete Time Control Design

The bilinear transformation provides a link between discrete time and continuous time systems. Assume that a discrete time plant model is given by $P_d(z)$. The corresponding discrete frequency response is obtained by substituting $z = e^{j\omega h}$, where h denotes the sampling time. The bilinear transformation is a conformal mapping and is defined as
$$w = \frac{az + b}{cz + d}, \tag{2}$$
where $a, b, c, d \in \mathbb{C}$, $ad \neq bc$, and w and z are complex indeterminates. If the complex planes are extended appropriately, the mapping (2) is one-to-one and onto and hence an unique inverse transformation exists. Setting $a = \frac{2}{h}$, $b = -\frac{2}{h}$, and $c = d = -1$ yields the Tustin transformation:
$$w = \frac{2(z-1)}{2(z+1)}, \; z = \frac{2 + hw}{2 - hw}. \tag{3}$$
Substitution of (3) into $P_d(z)$ yields $P_d(w)$. $P_d(w)$ is a non-physical system that has continuous time properties, *i.e.*, w resembles the Laplace variable s. Hence, the frequency response of $P_d(w)$ is obtained by substituting $w = j\nu$, where ν is a fictitious frequency. The Tustin transformation preserves:

1) McMillan degree,
2) stability,
3) the frequency response, *i.e.*, $P_d(w)|_{w=j\nu} = P_d(z)|_{z=e^{j\omega h}}$, where the frequency axis is rescaled by

$$\nu = \frac{2}{h}\tan\left(\frac{\omega h}{2}\right), \tag{4}$$

4) the $\mathcal{H}_\infty$-norm, which is a consequence of property 3.

Note that in [7] and [3] the bilinear transformation to solve the discrete time $\mathcal{H}_\infty$ control problem by using Property 4. In this paper, use is made of Property 3 for design purposes.

B. Design Procedure

A stepwise procedure is given that enables the iterative design of high-performance discrete time controllers. The corresponding discrete time standard plant is depicted in Fig. 2. The discrete time signals in Fig. 2 are defined similarly as in Fig. 1 and are denoted by Greek symbols.

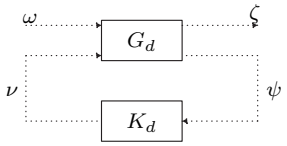

Fig. 2. Discrete time standard plant.

1) *Control goal and structure:* define the signals in Fig. 2. This step is similar to Step 1 in Section II-A.
2) *Plant modeling:* model the discrete time finite dimensional LTI system. Here, SI techniques can unambiguously be applied, since the data set and the model structure are both in the discrete time domain. Next, transform the discrete time model $P_d(z)$ into $P_d(w)$, see Section III-A. The model reduction tools of [26] can be applied, since $P_d(w)$ has continuous time properties.
3) *Control goal quantification:* quantify the control goal by means of frequency domain weighting filters. Since the bilinear transformation preserves the frequency response, it does not matter for the solution of the control problem whether the filters are defined in the z-plane or w-plane. However, the specification of loopshaping-based filters is more intuitive in the w-plane due to Bode's gain-phase relationship [5], *i.e.*, asymptotes can easily be determined. This fact was already observed in [13]. Note that true frequency ω should be translated to the fictitious frequency ν using (4).
4) *Model uncertainty quantification:* determine an uncertainty model in the w-plane. A common method to model uncertainty is to compute the maximum additive error between the plant model and the identified Frequency Response Function (FRF) on at a discrete number of frequencies. Then, this upper bound is fitted by a real-rational transfer function. In the discrete time case, both the plant model and the identified FRF are transformed into the w-plane. Next, the upper bound is fitted in the w-plane using continuous time tools [3].
5) *Controller synthesis:* using the plant $P_d(w)$ and the weighting filters in the w-plane, a standard plant is constructed in the w-plane. Then, an $\mathcal{H}_\infty$-optimal controller is computed in the w-plane using continuous time optimization algorithms, see [9] and [3]. If the order of the resulting controller is too high, reduce its order using the continuous time tools of [26].
6) *Controller transformation:* the controller, resulting from Step 5, should be transformed from the w-plane into the z-plane to enable discrete time implementation. This does not involve any approximation: if $K_d(w)$ satisfies certain frequency domain specifications in terms of the fictitious frequency ν, then $K_d(z)$ satisfies these frequency domain specifications in terms of the true frequency ω.

IV. Exploiting Sampled-Data Control Theory

The intersample behavior is not taken into account in the discrete time control design approach of Section III. It is well-known that several control design techniques deteriorate the intersample behavior, *e.g.*, due to the cancelation of sampling zeros [2]. The intersample behavior depends on the particular discrete time controller, the continuous time plant, and the exogenous signals present in the setup of Fig. 3. The key idea is to evaluate the intersample behavior using frequency domain tools. The sampled-data synthesis problem, *i.e.*, the design of a discrete time controller taking into account intersample behavior, is discussed first in Section IV-A. Concepts from Section IV-A are required for the introduction of the sampled-data analysis problem in Section IV-B.

A. Sampled-Data Synthesis

The sampled-data control design problem amounts to the design of a discrete time controller for a continuous time plant with AD and DA converters, see Fig. 3. Sampled-data control addresses the true control goal, since performance is evaluated in the continuous time domain for most industrial applications.

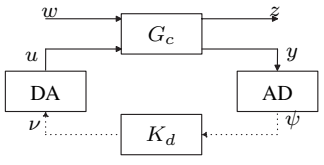

Fig. 3. Sampled-data standard plant.

The sampled-data system of Fig. 3 is Linear Periodically Time Varying (LPTV) if G_c and K_d are LTI. An important consequence is that the frequency separation principle is lost: if the exogenous input w consists of one frequency component ω_i, the output z contains the frequencies $\omega_i + l\omega_s$, $l \in \mathbb{Z}$, $\omega_s = \frac{2\pi}{h}$. Furthermore, the notion of transfer function does not apply for sampled-data systems and Bode diagrams cannot be made. This also implies that the worst-case $\mathcal{L}_2$-gain, *i.e.*, the $\mathcal{H}_\infty$-norm, may not be obtained for a sinusoidal

input signal of a single frequency. Hence, loopshaping based $\mathcal{H}_\infty$-design is not straightforward for sampled-data systems.

In [1], [27], an alternative definition is given for the FRF of sampled-data systems. This sampled-data FRF is also called the Robust Frequency Gain (RFG), see [15]. The key idea is to determine for each $\omega \in [0, \omega_s)$ the input signal in the set

$$\left\{ w(t) | w(t) = \sum_{l=-\infty}^{\infty} w_l e^{j\omega t + jl\omega_s t}, \|w_l\|_2 < \infty \right\}, \quad (5)$$

that leads to the largest $\mathcal{L}_2$-induced gain:

$$\mathrm{RFG}(j\omega) = \sup_{w \in \mathcal{L}_2} \frac{\|z\|_2}{\|w\|_2}. \quad (6)$$

The RFG is suitable for $\mathcal{H}_\infty$ loopshaping, since its peak value over frequency equals the $\mathcal{H}_\infty$-norm of the sampled-data system [27]. To study performance, however, it is desirable to evaluate the response of a sampled-data system to a sinusoidal input of a single frequency and not collect several frequencies as in (5). Hence, sampled-data loopshaping is not directly suitable for high performance motion control. Furthermore, including LTI uncertainty is not straightforward, see [10]. The alternative signal-based approach [20] is often too time-consuming in an industrial environment. This motivates the discrete time control design approach in Section III.

B. Sampled-Data Analysis and Multirate Extensions

The importance of Bode diagrams is well understood in industry, since the expected performance of a controller can easily be determined. For instance, many disturbances have a periodic, sinusoidal character. Hence, the disturbance attenuation properties of a controller for such disturbances can easily be determined from the closed-loop transfer functions. To investigate the intersample behavior of the sampled-data system of Fig. 3, the Performance Frequency Gain (PFG) [15], [6] is introduced. Assuming the input signal w is sinusoidal of a single frequency, the PFG is defined as

$$\mathrm{PFG}(j\omega) = \max_{w \neq 0} \frac{\|z\|_{\mathcal{P}}}{\|w\|_{\mathcal{P}}}, \quad (7)$$

where $\|s\|_{\mathcal{P}}$ is the power norm of a signal $s(t)$, defined as

$$\|s(t)\|_{\mathcal{P}} = \sqrt{\lim_{T \to \infty} \frac{1}{2T} \int_{-T}^{T} \|s(t)\|^2 dt} \quad (8)$$

This PFG leads to another definition of frequency response for sampled-data systems. The PFG involves an infinite summation. However, a closed-form computation method for the PFG is given in [15]. It can be observed that

$$\mathrm{PFG}(j\omega) \leq \mathrm{RFG}(j\omega). \quad (9)$$

Thus, in general the peak value of the PFG does not equal the $\mathcal{H}_\infty$-norm of a sampled-data system, which limits the use of the PFG for $\mathcal{H}_\infty$-loopshaping. However, the PFG is useful for frequency domain intersample behavior analysis, since it considers the response of sampled-data systems to sinusoidal input signals, similar to the Bode diagram for LTI systems.

To analyze intersample behavior, knowledge of the plant is required at a higher sampling frequency than the sampling frequency of the controller. Regarding the PFG and RFG, it is assumed that a continuous time model is available. This is an unrealistic assumption in industrial applications, see Section II-B. However, it is often possible to identify the plant at a higher sampling frequency $\omega_{s,h}$ than the controller sampling frequency $\omega_{s,l}$, where $\omega_{s,h} = F\omega_{s,l}$, $F = 2, 3, \ldots$, since SI is computationally less demanding than real-time control. For instance, a dedicated spectrum analyzer can be connected to the feedback control loop. The plant model at a higher sampling frequency $\omega_{s,h}$ can be interconnected with the controller at the low sampling frequency $\omega_{s,l}$ using an upsampler $\mathcal{S}_u$, zero-order-hold interpolator $\mathcal{I}_{ZOH}$, and downsampler $\mathcal{S}_d$ [23], instead of the usual AD and DA converters, see Fig. 4. The system in Fig. 4 is multirate and LPTV. Next, the PFG_h is defined as

$$\mathrm{PFG}_h(e^{j\omega \frac{2\pi}{\omega_{s,h}}}) = \max_{\omega_h \neq 0} \frac{\|\zeta_h\|_{\mathcal{P}}}{\|\omega_h\|_{\mathcal{P}}}, \quad (10)$$

where ω_h is assumed to be a sampled sinusoid of a single discrete frequency and the power norm of a discrete time signal σ is defined as

$$\|\sigma[k]\|_{\mathcal{P}} = \sqrt{\lim_{N \to \infty} \frac{1}{2N+1} \sum_{k=-N}^{N} \|\sigma[k]\|^2 dt}. \quad (11)$$

Contrary to the PFG, computation of the PFG_h for multirate systems only involves a finite summation.

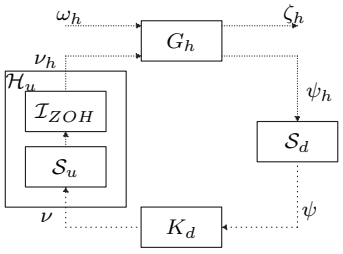

Fig. 4. Multirate standard plant.

V. Industrial Example

A controller is designed for a next-generation industrial wafer stage using the approach of Section III. Wafer stages are used for positioning a silicon disc (wafer) with respect to the imaging optics in wafer scanners. An extremely high position accuracy is required due to the fine patterns on the to be produced ICs. The design is improved iteratively to attenuate a particular disturbance. In this particular case, sampled-data analysis shows that the intersample behavior can be poor compared to the response of the system *at* the controller sampling instants.

The wafer stage is controlled in all six degrees-of-freedom. Interferometers with sub-nanometer accuracy are used for sensing. The system is rigid-body decoupled by appropriate

sensor and actuator placement and transformation. In the remainder of this section, only the vertical direction is considered. The other degrees-of-freedom are controlled by standard PID controllers.

A. Nominal control design

The discrete time control design procedure of Section III is briefly discussed for the wafer stage example.

1) *Control goal and structure:* a four-block problem is defined analogous to [25] and cast into the standard plant formulation of Fig. 2. The sampling frequency of the controller equals 1250 [Hz], hence the Nyquist frequency equals 625 [Hz].
2) *Plant modeling:* a FRF is identified at 1250 [Hz] and a 10^{th} order model $P_d(z)$ is estimated using [14]. This model is transformed in the w-plane, see Fig. 5. A high order plant model is used, since the high-frequent parasitic dynamics limit the achievable performance and may endanger closed-loop stability.
3) *Control goal quantification:* weighting filters are defined in the w-plane based on loopshaping ideas, see [25] for the particular parametrization of the weighting filters.
4) *Model uncertainty quantification:* not addressed.
5) *Controller synthesis:* an $\mathcal{H}_\infty$-suboptimal controller is computed using [3]. The resulting controller $K_{d,nom}(w)$ has 13 states due to the order of the weighting filters and the plant model.
6) *Controller transformation:* inverse transformation of $K_{d,nom}(w)$ into $K_{d,nom}(z)$, see Fig. 6, yields an implementable controller. It can be observed that $K_{d,nom}$ had a PID characteristic with high-frequent roll-off due to the particular choice of weighting filters.

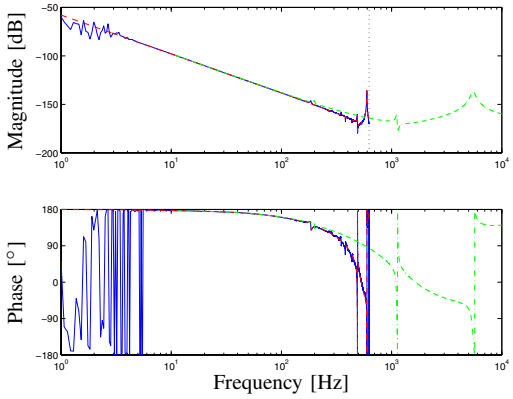

Fig. 5. Bode plot of plant: identified FRF at 1250 [Hz] (solid), $P_d(z)|_{z=e^{j\omega h}}$ (dashed), $P_d(w)|_{w=j\nu}$ (dash-dotted).

B. Error-based redesign

Fig. 7 shows experimentally obtained error signals using $K_{d,nom}$ during standstill, *i.e.*, the reference trajectory equals zero. The bottom figure depicts the Cumulative Power Spectrum (CPS) that gives the distribution of the signal power over frequency. The error signals are both extracted from the control loop at 1250 [Hz] and at 5000 [Hz]. The former is the signal that is available as input for the discrete time controller, whereas the latter is used to investigate the intersample behavior later on. There is a dominant (discrete time) frequency of 250 [Hz] in the 1250 [Hz] measurement. The weighting filters of Step 3 are modified to account for the measured error spectrum, see [24]. The resulting controller is called $K_{d,eb}$ and is also depicted in Fig. 6. The main difference with $K_{d,nom}$ is that $K_{d,eb}$ has a large peak around 250 [Hz]. The resulting error signal after implementation of $K_{d,eb}$ is depicted in Fig. 8. The 250 [Hz] component has effectively been removed from the error signal in the 1250 [Hz] measurement.

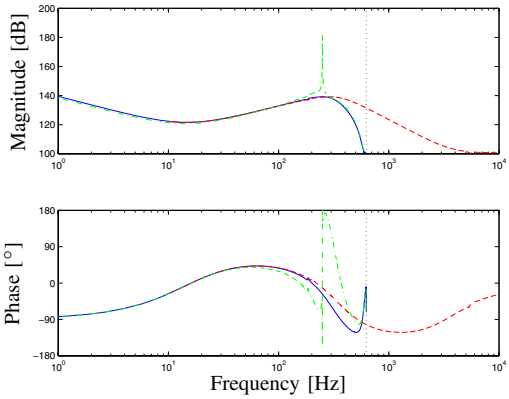

Fig. 6. Bode plot of $K_{d,nom}(z)|_{z=e^{j\omega h}}$ (solid), $K_{d,nom}(w)|_{w=j\nu}$ (dashed), $K_{d,eb}(z)|_{z=e^{j\omega h}}$ (dash-dotted).

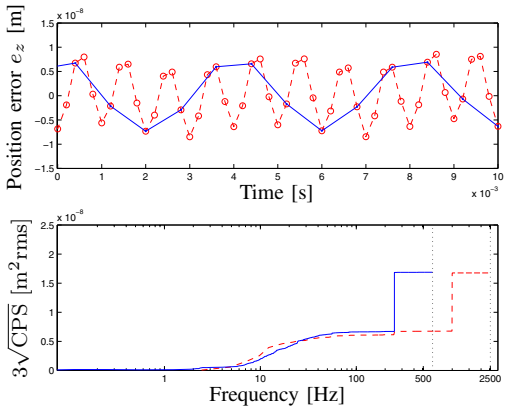

Fig. 7. Measured errors using $K_{d,nom}(z)$, sampling frequency 1250 [Hz] (solid), sampling frequency 5000 [Hz] (dashed).

C. Intersample analysis

In Section V-B, it is observed that $K_{d,eb}$ has effectively reduced the error signal *at* the controller sampling instants. However, when comparing Fig. 8 with Fig. 7, it can be observed that the system response *in between* the controller sampling instants has significantly deteriorated. Intuitively, this is best explained by the fact that the error signal of Fig. 7 contains aliased components: the discrete time controller is too slow to effectively attenuate such disturbances. If the true frequency of the disturbance was at 250 [Hz], the disturbance would have effectively been attenuated. This can be observed from $\text{PFG}_h(e^{j\omega\frac{2\pi}{\omega_{s,h}}})$, see Fig. 9, where a discrete time plant

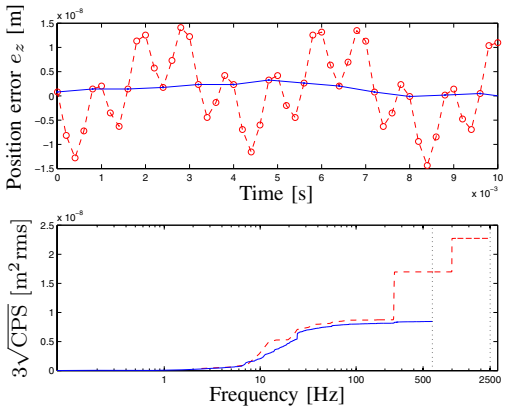

Fig. 8. Measured errors using $K_{d,eb}(z)$, sampling frequency 1250 [Hz] (solid), sampling frequency 5000 [Hz] (dashed).

model with sampling frequency $\omega_{s,h} = 5$ [kHz] is used. Plant output disturbances are considered as exogenous inputs. From Fig. 9, it can be observed that sinusoidal disturbances with a frequency of 250 [Hz], the power of at output is reduced by 28.4 [dB] compared to the input power. At 1000 [Hz], the power of the output is increased by 2.85 [dB] compared to the input power. Qualitatively, this corresponds with Fig. 7 and Fig. 8. No quantitative results should be drawn from Fig. 7 and Fig. 8, since the measurement time is rather short. It is concluded that discrete time control design involves a tradeoff between the primary frequency band and the complementary bands. Furthermore, poor intersample behavior is not always detectable from measurements in the discrete time feedback control loop.

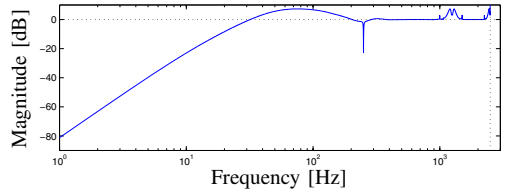

Fig. 9. Bode magnitude plot of $\text{PFG}_h(e^{j\omega\frac{2\pi}{\omega_{s,h}}})$, see Fig. 4.

VI. Conclusions

A control design approach is proposed that extends a present industrial design practice in the sense that the digital controller implementation is explicitly addressed. Since no approximations are involved in the control design procedure, higher performance can be achieved compared to continuous time control design with *a posteriori* controller discretization.

The intersample behavior issue is covered by an *a posteriori* intersample behavior analysis and iterative redesign of the discrete time controller. The intersample behavior analysis requires knowledge of the plant in between the controller sampling instants. The PFG is extended to the multirate case, since accurate modeling of continuous time systems from sampled data is hard. A discrete time model of the plant that operates at a higher sampling frequency than the controller sampling frequency suffices for the computation of the PFG_h. Experimental results demonstrate the effectiveness of the proposed design approach and illustrate the importance of intersample behavior.

References

[1] M. Araki, Y. Ito, and T. Hagiwara. Frequency response of sampled-data systems. *Automatica*, 32(4):483–497, 1996.

[2] K. J. Åström, P. Hagander, and J. Sternby. Zeros of sampled systems. *Automatica*, 20(1):31–38, 1984.

[3] G. J. Balas, J. C. Doyle, K. Glover, A. Packard, and R. Smith. *μ-Analysis and Synthesis Toolbox*. The MathWorks, Inc., Natick, Massachusetts, third edition, 2001.

[4] B. A. Bamieh and J. B. Pearson. A general framework for linear periodic systems with applications to $\mathcal{H}_\infty$ sampled-data control. *IEEE Trans. Automat. Contr.*, 38(5):717–732, 1992.

[5] H. W. Bode. *Network Analysis and Feedback Amplifier Design*. Van Nostrand, London, United Kingdom, 1945.

[6] M. W. Cantoni and K. Glover. Frequency-domain analysis of linear periodic operators with application to sampled-data control design. In *Proc. Conf. Dec. and Contr.*, pages 4318–4323, San Diego, California, 1997.

[7] T. Chen and B. A. Francis. *Optimal Sampled-Data Control Systems*. Springer, London, Great Britain, 1995.

[8] T. Chen and D. Miller. Reconstruction of continuous-time systems from their discretizations. *IEEE Trans. Automat. Contr.*, 45(10):19141917, 2000.

[9] J. C. Doyle, K. Glover, P. P. Khargonekar, and B. A. Francis. State-space solutions to standard $\mathcal{H}_2$ and $\mathcal{H}_\infty$ control problems. *IEEE Trans. Automat. Contr.*, 34(8):831–847, 1989.

[10] G. Dullerud. *Control of Uncertain Sampled-Data Systems*. Birkhauser Verlag, Boston, Massachusetts, 1995.

[11] G. F. Franklin, J. D. Powell, and M. Workman. *Digital Control of Dynamic Systems*. Addison Wesley Longman, Menlo Park, California, third edition, 1998.

[12] P. A. Iglesias and K. Glover. State-space approach to discrete-time $\mathcal{H}_\infty$ control. *Int. J. Contr.*, 54(5):1031–1073, 1991.

[13] G. W. Johnson, D. P. Lindroff, and C. G. A. Nording. Extension of continuous data system design techniques to sampled-data control systems. *AIEE Trans.*, 74, 1955.

[14] E. C. Levy. Complex-curve fitting. *IRE Trans. Automat. Contr.*, 4(1):37–43, 1959.

[15] O. Lindgärde. *Frequency Analysis of Sampled-Data Systems Applied to a Lime Slaking Process*. PhD thesis, Chalmers University of Technology, Göteborg, Sweden, 1999.

[16] L. Ljung. *System Identification: Theory for the User*. PRT Prentice Hall Information and System Sciences. Prentice Hall, Upper Saddle River, New Jersey, second edition, 1999.

[17] L. Ljung and T. Glad. *Modeling of Dynamic Systems*. Prentice Hall, Englewood Cliffs, New Jersey, 1994.

[18] R. Pintelon, P. Guillaume, Y. Rolain, J. Schoukens, and H. van Hamme. Parametric identification of transfer functions in the frequency domain - a survey. *IEEE Trans. Automat. Contr.*, 39(11):2245–2260, 1994.

[19] N. K. Sinha and G. P. Rao. *Identification of Continuous-Time Systems*. Kluwer Academic Publishers, Dordrecht, The Netherlands, 1991.

[20] S. Skogestad and I. Postlethwaite. *Multivariable Feedback Control*. John Wiley & Sons, Chichester, United Kingdom, 1996.

[21] M. Steinbuch and M. L. Norg. Advanced motion control: An industrial perspective. *Eur. J. Contr.*, 4(4):278–293, 1998.

[22] G. Stix. Toward "point one". *Scientific American*, 272(2):72–77, 1995.

[23] P. P. Vaidyanathan. *Multirate Systems and Filter Banks*. Signal Processing Series. Prentice Hall, Englewood Cliffs, New Jersey, 1993.

[24] M. van de Wal, G. van Baars, and F. Sperling. Reduction of residual vibrations by $\mathcal{H}_\infty$ feedback control. In *MOVIC*, volume 2, pages 481–487, Sydney, Australia, 2000.

[25] M. M. J. Van de Wal, G. van Baars, F. Sperling, and O. H. Bosgra. Multivariable $\mathcal{H}_\infty/\mu$ feedback control design for high-precision wafer stage motion. *Contr. Eng. Pract.*, 10(7):735–755, 2002.

[26] P. M. R. Wortelboer. *Frequency-Weighted Balanced Reduction of Closed-Loop Mechanical Servo Systems: Theory and Tools*. PhD thesis, Delft University of Technology, Delft, The Netherlands, 1994.

[27] Y. Yamamoto and P. P. Khargonekhar. Frequency response of sampled-data systems. *IEEE Trans. Automat. Contr.*, 51(2):166–176, 1996.